Observation of Plasmon-Optic Phonon Coupled Modes in GaAs/AlGaAs Resonant Tunneling Structures via Acoustic Phonon Decay Products

M. Giltrow, A. Kozorezov, M. Sahraoui-Tahar, and J. K. Wigmore
School of Physics and Materials, Lancaster University, Lancaster, LA1 4YB, United Kingdom

J. H. Davies, C. R. Stanley, B. Vogel, and C. D. W. Wilkinson
Department of Electronics and Electrical Engineering, Glasgow University, Glasgow, G12 8QQ, United Kingdom
(Received 29 August 1994; revised manuscript received 23 January 1995)

Using a nanosecond pulse technique to detect acoustic phonon decay products, we have observed plasmon-optic phonon coupled modes excited by tunneling electrons in the heavily doped collector of a double barrier resonant tunneling structure. From steps observed in the bias voltage dependence of the detected phonon flux we inferred the coupled mode energies to be 50 and 30 meV . Both modes decayed predominantly via lattice rather than electronic processes. Their widths were unexpectedly narrow, the result we believe of spatial inhomogeneity of collector carrier concentration.

PACS numbers: 72.10.Di, 63.20.Kr, 71.45.Gm, 73.40.Kp

Energy loss of hot electrons injected into a cold Fermi gas is a topic of great current interest, particularly in the context of vertical tunneling structures [1,2]. The primary mechanism for energy loss is expected to be the excitation of plasmon-optic phonon coupled modes. Although these modes have been modeled theoretically [3,4] and their interaction with hot electrons calculated by several workers [5–7], there have been few experimental studies of their role in energy loss processes in heterostructures [8,9]. The nanosecond phonon pulse experiments reported here provide a direct confirmation of their excitation by injected hot carriers in a tunneling structure. By observation of the acoustic phonons generated through decay of the two coupled modes, we have been able to determine their energies, estimate their relative coupling strengths to the injected electrons, and infer the mechanism of their subsequent decay.

The double barrier resonant tunneling structures (DBRTS) used in these experiments were circular mesas 65 μm in diameter, fabricated from a molecular-beam-epitaxial- (MBE-) grown wafer with a growth sequence as follows, beginning from the substrate: 500 nm GaAs doped with $2 \times 10^{18}\,\mathrm{cm}^{-3}$ of Si, 50 nm GaAs with $1 \times 10^{17}\,\mathrm{cm}^{-3}$ Si, 2.5 nm undoped GaAs, 5.6 nm undoped $Al_{0.4}Ga_{0.6}As$, 5.0 nm undoped GaAs, 5.6 nm undoped $Al_{0.4}Ga_{0.6}As$, 2.5 nm undoped GaAs, 50 nm GaAs doped with $1 \times 10^{17}\,\mathrm{cm}^{-3}$ Si, and finally 300 nm GaAs doped with $2 \times 10^{18}\,\mathrm{cm}^{-3}$ Si. The substrate was (100) semi-insulating GaAs 480 μm thick. The $I(V)$ characteristic of a device is shown in Fig. 1. All the data were taken at bias voltages below the resonant tunneling peak, with the electrons tunneling towards the substrate. Voltage pulses of duration 10 ns were applied to the device, the transmitted amplitude being determined by calculating the impedance mismatch from the $I(V)$ characteristic.

Phonon pulse experiments probe the polarization and angular distribution of emitted phonons with high temporal and spatial resolution. Previous experiments involving horizontal conduction in heterostructures were reported by Chin *et al.* [10], Hawker *et al.* [11], and Wigmore *et al.* [12]. The present experiments are the first in vertical structures. Phonons were detected by 65 μm square superconducting aluminum bolometers (Fig. 1, inset) and signals were recorded by a 3 GHz digital boxcar system. The experiments were run directly in liquid helium at the transition temperature of the aluminum bolometers, around 1.4 K.

Typical data are shown in Fig. 2, taken along the [100] axis, and at an angle of 30° in the (011) plane. The longitudinal acoustic (LA) and transverse acoustic (TA) modes were of different relative amplitudes in the two directions. The dependence of the mode amplitudes on the bias voltage across the structure is shown in Fig. 3, normalized to current, and hence relating to energy loss per electron. The main features were as follows.

(1) The LA peaks in both directions were on average independent of bias voltage, and hence of the energy of the injected electrons.

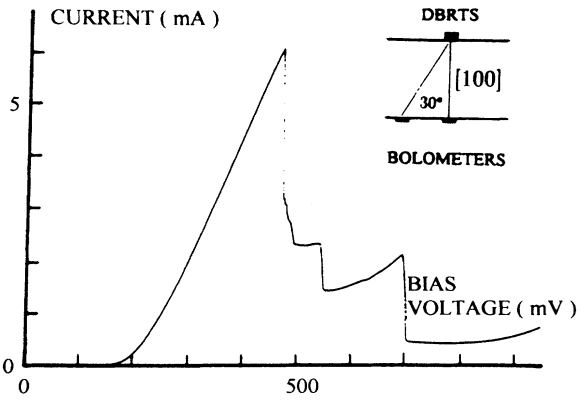

FIG. 1. Current-voltage characteristic of a DBRTS. Inset shows the experimental arrangement of device and bolometers.

 © 1995 The American Physical Society

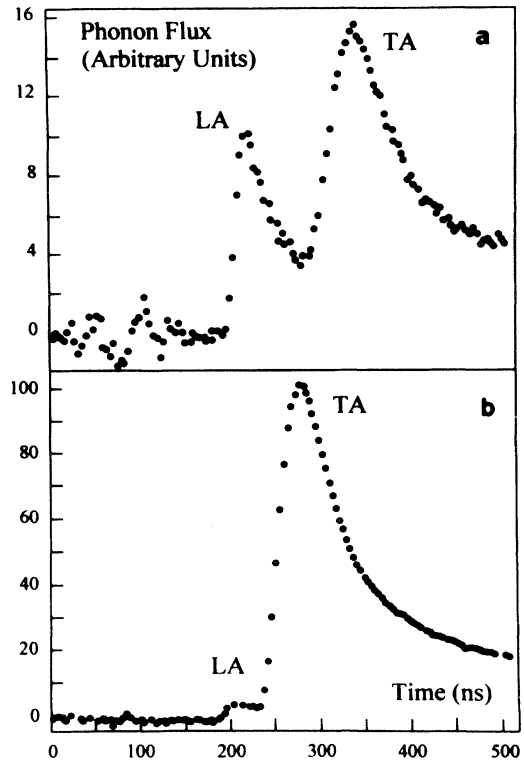

FIG. 2. Phonon flux detected by the two bolometers at (a) 30°, for (pulse) bias voltage 398 mV, and (b) 0° [100] for 325 mV. The exciting pulse occurred at 70 ns, followed by a burst of direct electromagnetic breakthrough.

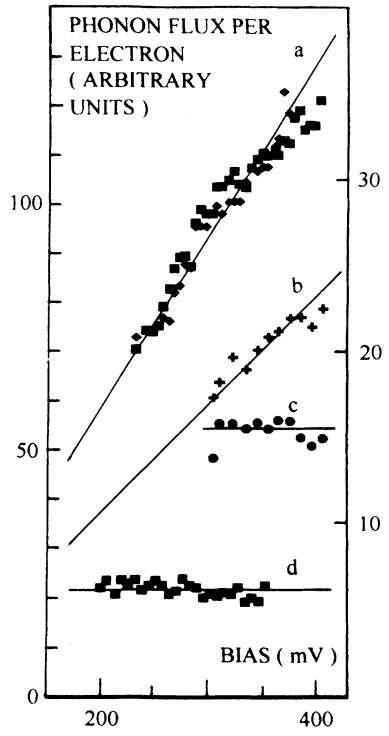

FIG. 3. Variation of phonon flux per electron as a function of bias voltage, (a) TA 0° (left hand scale), (b) TA 30°, (c) LA 30°, and (d) LA 0° (all right hand scale). The straight lines drawn through the two sets of TA data extrapolate to a bias voltage of 30 mV.

(2) In contrast, the TA modes for both orientations scaled with the energy of the tunneling electrons. The straight lines drawn in Fig. 3 extrapolate at zero phonon flux to a bias voltage of 30 mV .

(3) The small scale structure was reproducible from run to run, as shown in the expanded plot of the [100] TA data (Fig. 4). The detected phonon flux per electron followed a series of well-defined steps, with more or less equal heights. We took care to confirm that the structure was not an artifact of the bolometer response.

In analyzing the data, we note first that they are not consistent with the generation of heat by resistive dissipation in the contacts. Neither the fine structure observed nor the absence of bias voltage dependence of the LA modes could result from purely Ohmic heating. This result is not unexpected, since low resistance, Au/Ge/Ni Ohmic contacts of large area are easily made on heavily doped n^+ GaAs.

We find that all the features can be explained in terms of emission by the hot electrons of a cascade of plasmon-optic phonon coupled modes in the heavily doped collector of the structure. These modes subsequently decay into acoustic phonons which give rise to the observed bolometer signals. At a carrier concentration around $10^{18}\,\mathrm{cm}^{-3}$, the plasmonlike ($L+$) mode lies at higher energy and is more strongly coupled to the hot electrons than the phononlike ($L-$) mode [3,4]. It has been predicted [5–7] that excitation of these modes is the primary energy loss process for hot electrons injected into the Fermi gas. Rorison and Herbert [6] made detailed numerical calculations of the energy loss rates, concluding that coupled mode emission was an order of magnitude more probable than single-particle excitation. Our results suggest that a whole cascade of such modes is emitted in the process of hot electron thermalization.

Conditions for the existence of such a cascade have been discussed by Esipov and Levinson [13]. After the emission of one $L+$ (or $L-$) excitation the probability of a further mode being emitted remains greater than that of any other process, the "active region." Only when the energy of the hot electron has fallen below the threshold for excitation of the $L-$ mode can the single-particle excitation of the Fermi gas dominate (the "passive region"). The cascade process is illustrated in the inset to Fig. 4. The effect of changing the bias voltage across the structure is to vary the relative amounts of energy lost by an electron in the active and passive regions. The TA phonons reaching the bolometer result from down-conversion of the high frequency phonons emitted by the coupled modes, while the LA phonon flux arises from heating of the Fermi gas through single-particle excitations in the passive region. The latter does

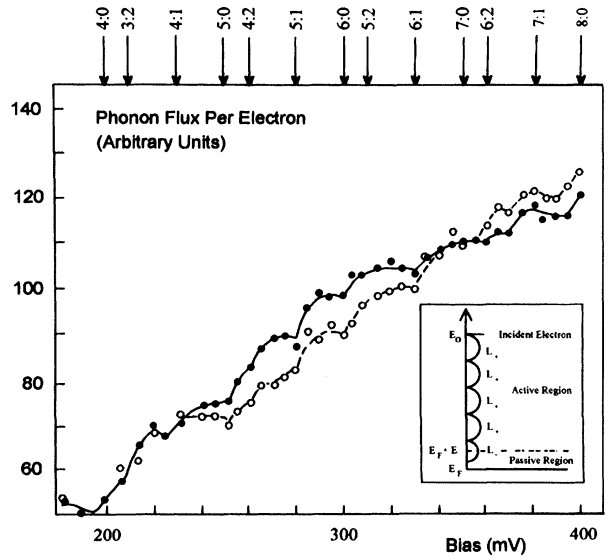

FIG. 4. TA 0° phonon flux per electron as a function of bias voltage. Two independent runs are shown to illustrate reproducibility. The numbers of $L+$ and $L-$ modes in different cascades are indicated above the arrows; the inset illustrates the 4 : 1 cascade.

not increase with bias voltage, because it is due only to residual energy of an electron below the $L-$ threshold, measured as 30 meV from our data. The conclusions are only slightly modified by the inclusion of secondary electrons excited by single-particle interactions of the initial hot electrons. These have energies well above the $L-$ threshold and hence also decay via coupled modes, making a further small contribution to Fermi gas heating in the passive region.

We estimated the maximum temperature T_e to which the Fermi gas may be heated through the deposition of 30 meV per electron. The usual asymptotic (analytic) approximations are not valid for our experimental conditions. Hence we transformed the expressions given by Kogan [14] into series expansions based on the solution in the degenerate limit, yielding an equation for the power input P per electron,

$$P = \sum_{m=1}^{\infty} \left\{ \frac{0.256}{m^5} T_e^5 \gamma\left[5; \frac{25.7m}{T_e}\right] + \frac{0.072}{m^3} T_e^3 \gamma\left[3; \frac{25.7m}{T_e}\right] \right\} \text{eV s}^{-1}. \quad (1)$$

Here $\gamma(n;\alpha)$ is an incomplete gamma function and screening is neglected. At the resonant tunneling peak $P = 4.5 \times 10^5\,\text{eV s}^{-1}$, yielding a maximum value for T_e of 22 K. This is well below the threshold for optic phonon emission. It should be noted also that if the energy loss were dominated by this process, the LA emission would be approximately independent of the tunneling current in contrast to observation. T_e will never fall to zero, since cascades occur which contain different numbers of $L+$ and $L-$ components with overlapping residual energies. Piezoelectric coupling excites both LA and TA phonons depending on crystallographic orientation; in the 30° direction both modes are emitted while at 0° both are absent. Deformation potential coupling gives rise to an isotropic LA component. At 22 K the deformation potential term is approximately 6 times the piezoelectric, and the maximum frequency of the emitted phonons is a few hundred GHz.

A further implication of the results is that the Fermi gas in the collector is heated *only* by the residual energy of injected electrons in the passive region. There is no heating through single-particle electronic interactions of the coupled modes in the active region, and hence we may infer that the coupled modes decay predominantly via lattice processes. Although collisional damping of coupled modes in heavily doped GaAs has been studied previously, for example, by Ramsteiner *et al.* [15], there has been no previous consideration of energy decay via lattice vibrations. The coupling mechanism through which this can occur is of the form $c_1u^3 + c_2Eu^2$, where u is the lattice displacement and E the electric field due to the coupled mode. For GaAs both c_1, due to anharmonicity, and c_2, the second-order dipole moment, are known [16]. Calculations give a value of below 1 ps for the energy decay time of the $L+$ mode directly into phonons by this process [17] with significant contributions from decay into LA + LA, LO + LA, LO + TA, and TO + LA channels.

The acoustic phonons thus created are of high frequency, and they decay very rapidly through anharmonicity. Our data indicate that only TA down-converted phonons reach the bolometer ballistically. In order to understand this new and important result, first we note that the maximum frequency of ballistic phonons in our sample is around 1 THz because of isotope scattering [18]. An LA phonon at this frequency would originate from a parent LA phonon at about 2 THz [19]. However, there are far fewer 2 THz LA phonons than TA because of their relative densities of states. Furthermore, the elastic scattering rate for LA $\rightarrow$ TA at 2 THz is several times faster than the spontaneous decay rate. Ballistic 1 THz TA phonons arise from decay of fast TA modes; the slow TA modes are nondecaying except following elastic mode conversion [20].

We may now understand the steps seen in the 0° TA data (Fig. 4). A step corresponds to the voltage at which the residual energy of an electron at the bottom of a decay cascade reaches the $L-$ threshold. Any additional energy then goes into coupled mode excitation and is no longer available for heating the Fermi gas. As the bias voltage is further increased, no additional increase in the 0° TA peak is possible until the residual energy is again large enough for excitation of a further coupled mode. Until this point is reached, the extra energy goes instead into heating the Fermi gas.

The values of the bias voltage at which the steps occur provide a direct determination of the multiples of $L+$ and $L-$ coupled modes that are excited by the

injected electrons. The observed features could be best fitted by taking energies for $L+$ and $L-$ of 50 ± 1 and 30 ± 1 meV. These values are consistent with a carrier density of $1.2 \times 10^{18}\,\mathrm{cm}^{-3}$, rather than the dopant level of $2 \times 10^{18}\,\mathrm{cm}^{-3}$, suggesting compensation. In Fig. 4 the arrows give the indicated multiple combinations of $L+$ and $L-$ modes. We note that the plasmonlike $L+$ mode dominates, while at most two phononlike $L-$ modes occur in the cascade. Since the emission of at least one $L-$ excitation is certain whenever the energy of an electron falls between 30 and 50 meV, the indication is that the $L+$ mode is several times more strongly coupled than the $L-$.

The sharpness of the observed steps implies that the coupled modes are only a few meV wide, between a minimum energy determined by conservation rules and a maximum limited by the entry of the mode into the Landau damping regime. To describe the latter, it is necessary to take into account the spatial inhomogeneity of carrier concentration in the collector. A description of plasmon behavior based on mean carrier density is valid only in the long wavelength limit, and a coupled mode will not propagate in regions where it is beyond the characteristic local cutoff. In our sample, we calculate that the $L+$ bandwidth is reduced by this mechanism to less than 5 meV, which is entirely consistent with Raman data [21] for a sample of concentration $1.25 \times 10^{18}\,\mathrm{cm}^{-3}$.

We are indebted to EPSRC, London for supporting both project and personnel (M. G. and A. K.).

[1] A. F. J. Levi, J. R. Hayes, P. M. Platzman, and W. Weigman, Phys. Rev. Lett. **55**, 2071 (1985).

[2] A. P. Long, P. H. Beton, and M. J. Kelly, Semicond. Sci. Technol. **1**, 63 (1986).

[3] B. B. Varga, Phys. Rev. **137**, A1896 (1965).

[4] M. E. Kim, A. Das, and S. D. Senturia, Phys. Rev. B **18**, 6890 (1978).

[5] J. F. Young and P. J. Kelly, Phys. Rev. B **47**, 6316 (1993).

[6] J. M. Rorison and D. C. Herbert, J. Phys. C **19**, 399 (1986); **19**, 6357 (1986).

[7] C. Peschke, J. Appl. Phys. **74**, 327 (1993).

[8] J. A. Kash, Phys. Rev. B **40**, 3455 (1989).

[9] C. L. Petersen and S. A. Lyon, Phys. Rev. Lett. **63**, 2849 (1989).

[10] M. A. Chin, V. Narayanamurti, H. L. Störmer, and J. C. M. Hwang, in *Phonon Scattering in Condensed Matter IV,* edited by W. Eisenmenger, K. Lassman, and S. Döttinger (Springer, Berlin, 1984), p. 328.

[11] P. Hawker, A. J. Kent, M. Henini, and O. H. Hughes, Solid State Electron. **33**, 1755 (1989).

[12] J. K. Wigmore, M. Erol, M. Sahraoui-Tahar, M. Ari, C. D. W. Wilkinson, J. H. Davies, M. C. Holland, and C. R. Stanley, Semicond. Sci. Technol. **6**, 839 (1991); **8**, 322 (1993).

[13] S. E. Esipov and Y. B. Levinson, Adv. Phys. **36**, 331 (1987).

[14] S. M. Kogan, Sov. Phys. Solid State **4**, 1813 (1963).

[15] M. Ramsteiner, J. Wagner, P. Hiesinger, and K. Köhler, J. Appl. Phys. **73**, 5023 (1993).

[16] C. Flytzanis, Phys. Rev. B **6**, 1264 (1972).

[17] A. G. Kozorezov and J. K. Wigmore (to be published).

[18] S. Tamura, Phys. Rev. B **30**, 849 (1984).

[19] S. Tamura, Phys. Rev. B **31**, 2574 (1985).

[20] H. J. Maris and S. Tamura, Phys. Rev. B **47**, 727 (1993).

[21] U. Nowak, W. Richter, and G. Sachs, Phys. Status Solidi (b) **108**, 131 (1981).